The Journal of Infectious Diseases

MAJOR ARTICLE

Functional Compartmentalization of Antibodies in the Central Nervous System During Chronic HIV Infection

Marianna Spatola,[1] Carolin Loos,[1,2] Deniz Cizmeci,[1,2] Nicholas Webb,[1] Matthew J. Gorman,[1] Evan Rossignol,[1] Sally Shin,[1] Dansu Yuan,[1] Laura Fontana,[1] Shibani S. Mukerji,[3] Douglas A. Lauffenburger,[2] Dana Gabuzda,[4,a,©] and Galit Alter[1,a]

[1]Ragon Institute of Massachusetts General Hospital, Massachusetts Institute of Technology, and Harvard, Cambridge, Massachusetts, USA; [2]Massachusetts Institute of Technology, Cambridge, Massachusetts, USA; [3]Massachusetts General Hospital, Boston, Massachusetts, USA; and [4]Dana Farber Cancer Institute, Boston, Massachusetts, USA

The central nervous system (CNS) has emerged as a critical HIV reservoir. Thus, interventions aimed at controlling and eliminating HIV must include CNS-targeted strategies. Given the inaccessibility of the brain, efforts have focused on cerebrospinal fluid (CSF), aimed at defining biomarkers of HIV-disease in the CNS, including HIV-specific antibodies. However, how antibodies traffic between the blood and CNS, and whether specific antibody profiles track with HIV-associated neurocognitive disorders (HAND) remains unclear. Here, we comprehensively profiled HIV-specific antibodies across plasma and CSF from 20 antiretroviral therapy (ART) naive or treated persons with HIV. CSF was populated by IgG1 and IgG3 antibodies, with reduced Fc-effector profiles. While ART improved plasma antibody functional coordination, CSF profiles were unaffected by ART and were unrelated to HAND severity. These data point to a functional sieving of antibodies across the blood-brain barrier, providing previously unappreciated insights for the development of next-generation therapeutics targeting the CNS reservoir.

Keywords. cerebrospinal fluid; plasma; antibody functions; complement deposition; phagocytosis; NK activation; Fc receptors; ART; HIV-associated neurocognitive disorders.

Acute human immunodeficiency virus (HIV) infection is marked by a rapid burst of systemic viral replication, seeding diverse tissues, including the central nervous system (CNS) [1]. Detection of HIV-RNA within the cerebrospinal fluid (CSF) has been used as evidence of viral infection in the brain [2, 3]. However, whether this represents active infection of CNS resident cells or passage of infected cells remains unclear. Progression of HIV-associated neurocognitive disorders (HAND), despite systemic viral suppression by antiretroviral therapy (ART) [4, 5], has been proposed to be caused by productive infection of brain-resident cells. Moreover, although increased levels of some inflammatory chemokines decline in blood following ART, they remain elevated in CSF [6–9], suggesting the persistence of a neuroinflammatory environment.

Beyond elevated inflammatory chemokines in the CSF, emerging data suggest the importance of virus-specific antibodies as critical biomarkers of disease. Specifically, persistence of high CSF HIV antibodies has been proposed as an indicator of ongoing viral replication in the CNS [10]. However, whether CSF antibodies are transferred from blood and whether they are functionally compartmentalized remains unclear. Here, we applied systems serology to comprehensively dissect humoral immune profiles in the plasma and CSF of chronically infected persons with HIV. Striking brain-specific antibody signatures were identified, marking unique compartmentalization of the humoral response within the CNS.

METHODS

Participants, and Clinical and Biological Markers

Paired plasma and CSF were collected between 2004 and 2012 from 20 persons with HIV infected for less than 5 years: 9 were ART naive, and 11 were virally suppressed (HIV-RNA <200 copies/mL) on ART. Participants were identified from the CNS HIV Antiretroviral Therapy Effects Research (CHARTER) study, which aimed to determine the frequency of HAND in a prospective cohort of over 1000 persons with HIV [11]. All participants provided written informed consent and underwent clinical evaluation, routine laboratory tests (no information about CSF oligoclonal bands was available), and neuropsychological testing. HAND severity was classified based on the Frascati criteria [11, 12] (asymptomatic neurocognitive impairment [ANI], mild neurocognitive disorder [MND], and HIV-associated dementia [HAD]), and assessed using Global Clinical Rating and demographically corrected cognitive test

Received 13 September 2021; editorial decision 05 April 2022; accepted 07 April 2022; published online 13 April 2022

[a]D. G. and G. A. contributed equally.

Correspondence: Galit Alter, PhD, Ragon Institute of MGH, MIT, and Harvard Medical School, 400 Technology Square, Cambridge, MA 02139 (galter@mgh.harvard.edu).

The Journal of Infectious Diseases® 2022;226:738–50

https://doi.org/10.1093/infdis/jiac138

scores (T-scores) [12, 13]. A conversion table from T-scores to clinical rating has been previously defined [13].

Antibody Assays

Paired plasma and CSF samples were used for antibody testing, in a blinded fashion. Results were obtained from duplicates and by averaging 2 independent experiments. Antibody assays included measurements of pathogen-specific antibody isotype/subclass levels, binding capacity to Fc-receptors (FcRs) and complement, and ability to drive antibody-effector functions, as described below. For all assays, events were detected using a Bio-Plex System (IntelliCyt, iQue Screener Plus).

Selection of HIV Antigens and Controls

Antibody responses to 3 different HIV antigens (gp120, IT-001-0024p; gp140, IT-001-0024TMp; and p24, IT-001-020p; ImmuneTech) and non-HIV antigens (herpes simplex virus 1 [HSV1], IT-005-055p; HSV2, IT-005-011p; Epstein-Bar virus [EBV], IT-005-035p, ImmuneTech; cytomegalovirus [CMV], CMV-PENT-100; Cederlane) were assessed. Influenza virus A (IT-003-SW12p and IT-003-001p; ImmuneTech) and Ebola (0501-015; IBT) were used as a positive and negative controls, respectively.

Isotype, Subclass, FcR/Complement Binding Analysis

HIV-specific and other pathogen-specific antibody isotype, subclasses, and FcR-binding and complement-binding capacity were measured using a customized multiplexed Luminex assay, as reported [14]. Briefly, HIV or control antigens were coupled to fluorescent carboxyl-modified microspheres, then incubated with plasma (dilution 1:100) or CSF (dilution 1:10). Immunocomplexes were then washed and incubated with a phycoerythrin (PE)-conjugated anti-human antibody (IgM [9020-09], IgA1 [9130-09], IgA2 [9140-09], total IgG [9040-09], IgG1 [9052-09], IgG2 [9070-09], IgG3 [9210-09], IgG4 [9200-09]; Southern Biotech). Similarly, for assessment of binding capacity to FcR or complement, recombinant human FcαR, FcγRIIa, FcγRIIb, FcγRIIIa, FcγRIIIb, FcRn, and C1q (Duke Protein Production Facility) were biotinylated, conjugated to streptavidin-PE, and incubated with the immunocomplexes. Median fluorescence intensity (MFI) was reported and compared to phosphate-buffered saline levels.

Determination of Antibody-Mediated Functions

1. Antibody-dependent cellular phagocytosis (ADCP) and neutrophil phagocytosis (ADNP) were assessed using a flow cytometry, microsphere-based phagocytic assay, as described [15, 16]. Briefly, HIV or control antigens were biotinylated and coupled to yellow-green fluorescent neutravidin microspheres (F8776; Thermo Fisher), then incubated with plasma or CSF (dilution 1:100 and 1:10, respectively). Microspheres-bound immunocomplexes were then washed and incubated with a human monocyte cell line (THP-1) to assess ADCP or with human neutrophils obtained from healthy donors' blood to assess ADNP. Cells in ADNP assays were then stained with anti-Cd66b Pac blue antibody (305112; BioLegend) to identify $CD66b^+$ neutrophils. In both ADCP and ADNP assays cells were fixed with 4% paraformaldehyde (PFA) and identified by gating on single cells and microsphere-positive cells. Microsphere uptake was quantified as a phagocytosis score, calculated as the (percentage of microsphere-positive cells) × (MFI of microsphere-positive cells) divided by 100 000.
2. Antibody-dependent complement deposition (ADCD) assessed the ability of antigen-specific antibodies to bind complement component C3b [17], as described [18]. Briefly, HIV or control antigens were biotinylated, coupled to red fluorescent neutravidin microspheres (F8775; Thermo Fisher), and then incubated with plasma or CSF samples (dilution 1:30 or 1:3, respectively). Immune complexes were washed, incubated with guinea pig complement (CL4051; Cedarlane), then washed with 15 mM EDTA. Complement deposition was detected by fluorescein-conjugated goat IgG to guinea pig complement C3b (855385; MP Biomed) and analyzed gating on single microspheres and $C3b^+$ events.
3. Antibody-dependent natural killer cell activation (ADNKA) quantified the ability of antigen-specific antibodies to activate human NK cells to produce CD107α, IFN-γ, and CCL4 (MIP-1β), as described [19]. Briefly, enzyme-linked immunosorbent assay (ELISA) plates were coated with HIV or control antigens. NK cells were isolated from buffy coats, obtained from healthy blood donors, using RosetteSep NK enrichment kit (15065; Stem Cell Technologies), and rested overnight with interleukin 15 (IL-15), as reported [20]. Antigen-coated ELISA plates were then incubated with plasma or CSF (dilution 1:100 or 1:10, respectively). NK cells were stained with anti-CD107a (555802; BD) and treated with a protein-transport inhibitor (554724; BD Bioscience), and with brefeldin A (B7651; Sigma) to block degranulation. NK cells were then added to the immunecomplexes, labeled with surface staining including anti-CD3 (558117; BD), anti-CD16 (557758; BD) and anti-CD56 (557747; BD), washed, fixed with 4% PFA and permeabilized with PERM A/B (GAS001S100; Thermo Fisher) to allow intracellular staining with anti-IFNγ (340449; BD), and anti-CCL4 (550078; BD). NK cells were identified as $CD3^-CD56^+$ cells, and activation was defined as $CD107^+IFN\gamma^+CCL4^+$.

Statistical Analyses

Univariate comparative analyses of antibody features between groups or compartments were performed using nonparametric tests (Mann-Whitney, Kruskal-Wallis, and Friedman test) or

Table 1. Clinical Features, Demographics, and Laboratory Results of 20 Persons With HIV in the Study Cohort

Characteristic	All	ART Treated	Untreated	*P*
No. of individuals	20	11	9	
Age, y	35.3 (31.5–44.3)	34.8 (30.5–40.8)	36 (33.1–46)	.33
Sex, female, %	3/20 (15)	1/11 (9)	2/9 (22)	.56
Ethnicity, %				
White	11/20 (55)	6/11 (55)	5/9 (56)	1
Black	4/20 (20)	2/11 (18)	2/9 (22)	
Hispanic	3/20 (15)	2/11 (18)	1/9 (11)	
Other	2/20 (10)	1/11 (9)	1/9 (11)	
Education, y	14 (12–15.7)	14 (11–16)	14 (12.5–15)	.95
HIV infection duration, y	2.6 (0.6–3.3)	3.1 (2.6–4)	0.6 (0.4–2.2)	**.008**
ART duration, mo	…	24.2 (14.4–34.9)	…	
Plasma HIV copies/mL[a]	72.5 (40–24280.5)	40 (40–40)	29300 (524–93324)	**.0002**
CSF HIV copies/mL[a]	40 (40–460)	40 (40–40)	469 (181.5–5655)	**.003**
CSF/plasma viral load ratio	0.75 (0.1–1)	1 (0.1–1)	0.06 (0.02–0.33)	**<.0001**
Blood $CD4^+$ T cells, cells/mL	653 (477–876)	734 (630–115)	469 (245–728)	**.009**
Blood $CD4^+$ T-cell nadir, cells/mL	290 (229–515)	300 (269–533)	279 (198–484)	.37
CSF findings				
Total protein, mg/dL	34 (27–45.2)	34 (32.5–44.5)	33 (24–47)	.56
White blood cell count/mL	3 (2–6.7)	2 (1–3)	7 (2.5–9.5)	**.01**
Cognitive assessments[b]				
Global Clinical Rating	3 (1–4)	2 (1–4)	3 (2.5–5)	.09
Global Cognitive T Score	48.6 (45.7–53.7)	48.8 (46.6–56.4)	47.8 (45.3–51.1)	.5
HAND, %				
Neurocognitively unimpaired	13/20 (65)	8/11 (73)	5/9 (56)	.36
Neurocognitively impaired (asymptomatic or mild)	7/20 (35)	3/11 (27)	4/9 (44)	

Median and interquartile range are reported for continuous variables. Statistics were performed with Graph-Prism using Mann-Whitney test or 2-tailed Fisher exact test; bold indicates statistically significant differences ($P < .05$).

Abbreviations: ART, antiretroviral therapy; CSF, cerebrospinal fluid; HAND, HIV-associated neurocognitive disorder.

[a]Limit of HIV detection is 40 copies/mL.

[b]Cognitive function was assessed using Global Clinical Rating, which defines a deficit score ranging from 1 (no impairment) to 9 (Severe impairment), and demographically corrected Global Cognitive Test Scores (T-Scores), in which higher scores correspond to better cognitive performance [12, 13].

Spearman coefficients in GraphPad Prism with corrections for multiple comparisons.

Multivariate analyses were performed with R software, version 4.0.0. Luminex data were $\log_{10}$-transformed. All data were z-scored. Missing values were imputed using R package "DMwR." A multilevel partial least square discriminant analysis (M-PLSDA) with least absolute shrinkage selection operator (LASSO) was used to select antibody features that contributed most to discriminate plasma versus CSF antibodies [21]. Antibody features were ranked according to their variable importance in projection, for which higher values indicate higher contribution to the model. Five-fold cross validation was performed. The model was validated by comparing it to a null model, for which the modeling approach was repeated 100× with random shuffling of labels (for a total of 10 replicates of cross validation).

RESULTS

Clinical Characteristics

We profiled plasma- and CSF-derived antibodies from a cohort of 20 persons with HIV. Demographics, laboratory values, and clinical and neurocognitive assessments are shown in Table 1. Demographics were similar between the 9 ART-naive and 11 ART-treated individuals, with expected differences in plasma and CSF HIV-RNA levels, $CD4^+$ counts, and CSF white blood cell counts (Table 1).

Distinct HIV-Specific Antibody Profiles Across Plasma and CSF

HIV-specific IgG targeting gp120, gp140, and p24 were detected in both plasma and CSF (Figure 1A). However, although all Ig isotypes (IgG, IgM, and IgA) and subclasses (IgG1, IgG2, IgG3, and IgG4, and IgA1 and IgA2), were detected in plasma (Figure 1B–1D, data not shown for IgA), CSF was populated mainly by IgG1 and IgG3 (Figure 1B and 1D), with little IgM (Figure 1C). These data show compartmentalization of antibodies with specific IgG subclasses, and absence of IgM, within the CSF. Generally, antibodies in the CSF are thought to be primarily translocated from (and recycled to) the peripheral circulation via neonatal Fc receptor (FcRn)-mediated transport across the blood-brain barrier (BBB) [22–24]. Alternatively, in disease settings, CSF-antibodies may derive from circulating B cells that gain access to the brain and mature to antibody-

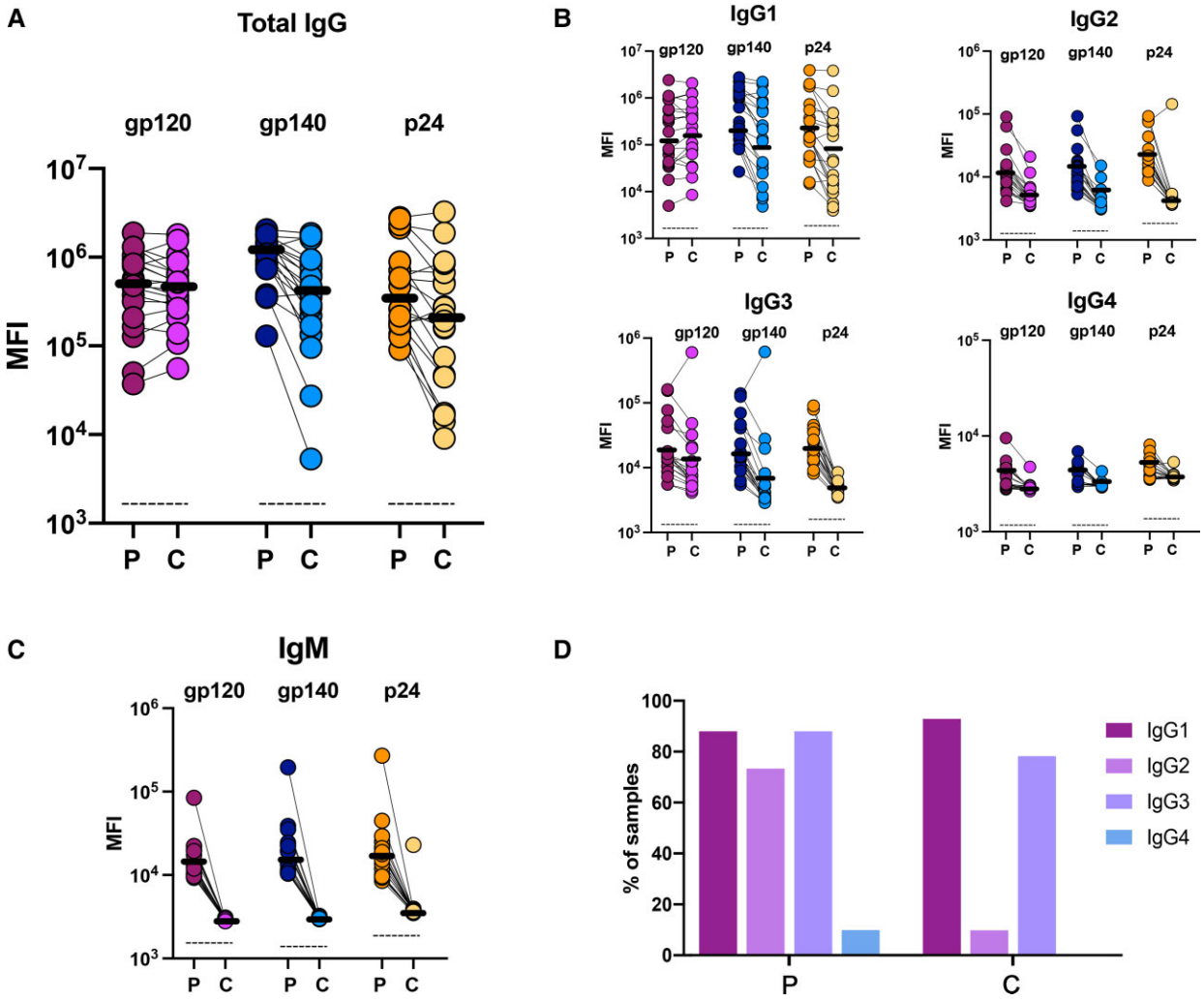

Figure 1. HIV-specific antibody classes and subclasses in plasma and CSF. *A–C*, Dot-line plot showing the level of total IgG antibodies, IgG subclasses (IgG1, IgG2, IgG3, IgG4), and IgM for plasma(P):CSF(C) pairs across 3 HIV antigens (gp120, gp140, p24). Horizontal lines indicate the average value in each compartment for each antigen. Dotted lines represent PBS background level. *D*, Bar plot indicating percentage of participants/samples with positive gp120-specific antibody responses of each IgG subclass in plasma and CSF. Positive responses were considered if MFI of each sample was 2-fold higher than the median MFI of PBS level (background) for each specific antigen. Abbreviations: CSF, cerebrospinal fluid; HIV, human immunodeficiency virus; Ig, immunoglobulin; MFI, median fluorescence intensity; PBS, phosphate-buffered saline.

producing plasma cells [25–27]. Thus, our data suggest that HIV-specific antibodies are unlikely to be produced within the CNS, as more variation in isotype and classes would be expected. It is possible that the restricted Ig isotypes and classes observed in the CSF may result from IgG subclass selectivity by FcRn (IgG1 > IgG4 > IgG3 > IgG2) [28, 29], and might explain why IgG1 and IgG3 predominated in CSF, whereas IgG2 and IgM were not detected.

HIV-Specific Antibodies Are Enriched in CSF Compared to Non-HIV–Specific Antibodies

To determine whether the observed Ig isotype/subclass exclusion from the CSF was unique to HIV-specific antibodies, or reflected overall differences in humoral compartmentalization across plasma and CSF, we analyzed antibody responses to several additional viruses (influenza virus, HSV1, HSV2, CMV, and EBV) in the same cohort. While diverse isotype/subclass antibody profiles were observed across other virus-specific responses in plasma, CSF antibodies were dominated again by a focused IgG1 response (Figure 2A). However, CSF to plasma ratios for individual IgG isotype/subclasses or IgM highlighted the presence of higher ratios of HIV-specific (all antigens combined) antibodies in CSF, especially for IgG1 (Figure 2B), pointing to an enrichment of HIV-specific compared to other virus-specific antibodies in the CSF. These data are in line with previous observations of persistently high anti-HIV responses in the CSF of persons with HIV [10].

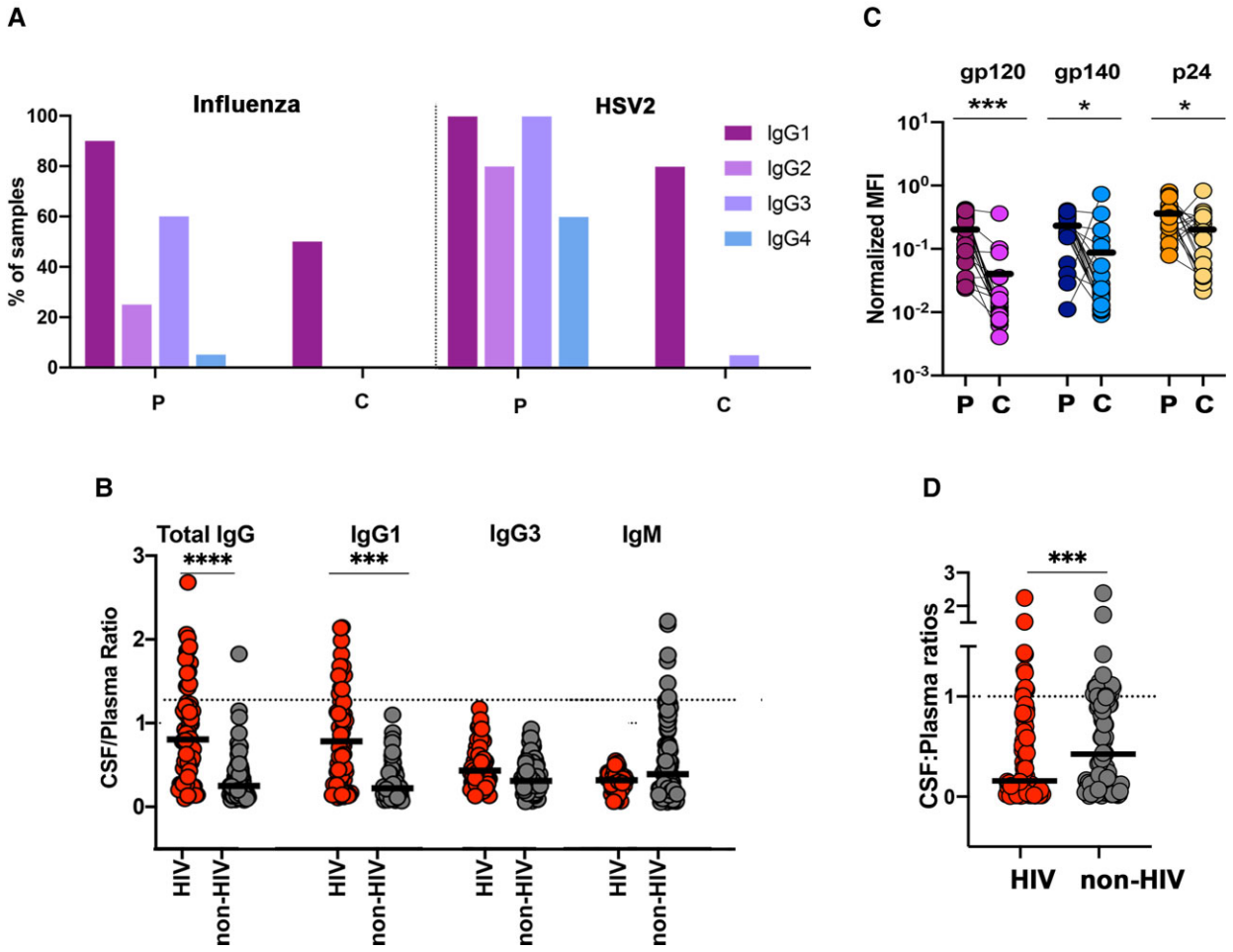

Figure 2. HIV-specific versus non-HIV–specific antibody subclasses and FcRn binding. *A*, Bar plot indicating percentage of participants/samples with positive influenza- or HSV2-specific antibody responses of each IgG subclass in plasma (P) and CSF (C). Responses were considered positive if MFI of each sample was 2-fold higher than the median MFI of phosphate-buffered saline level (background) for each specific antigen. *B*, Dot plot showing CSF:plasma ratios of total IgG, IgG1, IgG3, and IgM for antibodies to HIV (all antigens combined) versus non-HIV viruses (influenza, HSV1, HSV2, CMV, EBV combined). *C*, Dot-line plot showing FcR binding of HIV-specific antibodies (gp120, gp140, p24) for plasma:CSF pairs, after normalization by total HIV-specific IgG titer in each compartment. Horizontal black lines indicate the average value in each compartment for each antigen. *D*, Dot plots showing CSF:plasma ratios of binding to FcRn by HIV-specific antibodies (gp120, gp140, and p24-specificity combined) and non-HIV antibodies (influenza, HSV1, HSV2, CMV, EBV). *B–D*, Friedman test with Dunn correction, ****$P < .0001$, ***$P < .001$, *$P < .05$). Abbreviations: CSF, cerebrospinal fluid; CMV, cytomegalovirus; EBV, Epstein-Barr virus; FcRn, neonatal Fc receptor; HIV, human immunodeficiency virus; HSV, herpes simplex virus; Ig, immunoglobulin; MFI, median fluorescence intensity.

Weak CSF HIV-Specific Antibody Binding to FcRn Suggests Reduced Brain Clearance and Antibody Retention

We next aimed to assess whether the observed CSF-specific antibody-subclass profiles were related to differences in FcRn binding capacity by HIV or other pathogen-specific antibodies. FcRn binding was corrected for total pathogen-specific antibody titers to capture qualitative as well as quantitative differences. We observed strong FcRn binding by HIV-specific plasma antibodies, in contrast to weaker binding by CSF-antibodies (Figure 2C). Interestingly, HIV-specific CSF to plasma FcRn binding ratios were lower than those for influenza virus, HSV1, HSV2, CMV, and EBV (Figure 2D), and these differences were mainly driven by herpes viruses, and in particular CMV and EBV (Supplementary Figure 1). Overall, these data suggest selective retention within the CNS of HIV-specific antibodies (but not antibodies to other viruses) through reduced FcRn-mediated clearance in the context of active HIV disease.

CSF HIV-Specific Antibodies Are Less Functional Than Those in Plasma

To further understand the level of sieving across the compartments, we next explored the functional characteristics of HIV-specific antibodies across the plasma and CSF. Specifically, we explored differences in the capacity of HIV-specific antibodies to interact with diverse FcRs and to drive antibody-mediated functions (ADCD, ADCP, ADNP, and ADNKA). Given that IgG1 and IgG3 are the most

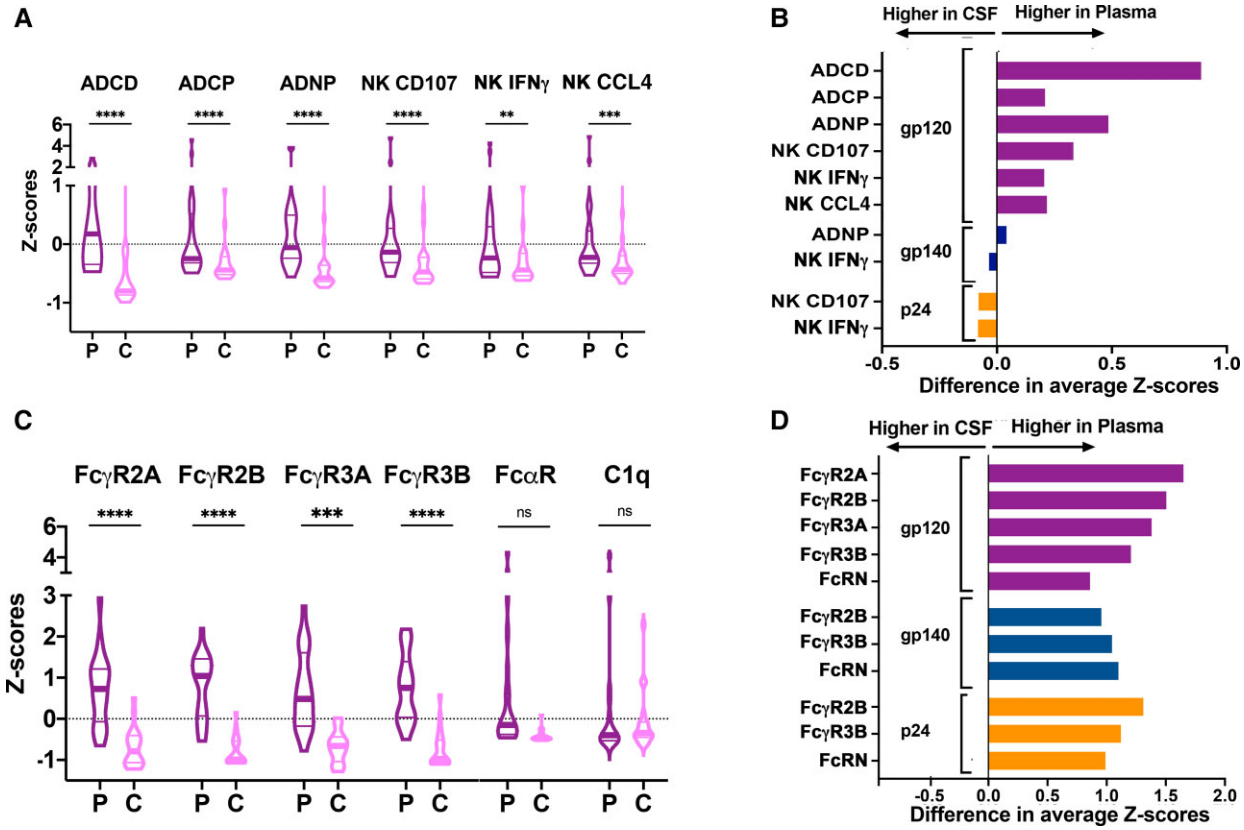

Figure 3. Antibody signatures in plasma and CSF. *A*, Violin plots of gp120-specific antibody functions in plasma (P) and CSF (C), including ADCD, ADCP, ADNP, and antibody-dependent NK cell activation with expression or production of CD107 (NK CD107), IFN-γ (NK IFN-γ), and CCL4 (NK CCL4). *B*, Bar plots of mean differences in antibody functions between plasma and CSF, across all 3 HIV antigens (gp120, gp140, p24). Bars on the right (or left) show features higher in plasma (or CSF). Only difference in mean between groups that are statistically significant ($P < .05$) are plotted. *C*, Violin plots of Fc receptor binding for gp120-specific antibodies in plasma (P) and CSF (C), including Fcγ receptors (FcγR2A, FcγR2B, FcγR3A, FcγR3B), Fcα receptor (FcαR), and binding to complement component C1q. *D*, Bar plots of mean differences in antibody binding to Fc receptors between plasma and CSF, across all 3 HIV antigens (gp120, gp140, p24). Bars on the right (or left) show features higher in plasma (or CSF). Only difference in mean between groups that are statistically significant ($P < .05$) are plotted. *A–D*, normalized values, Z-scores, Friedman test with Dunn correction, $^{**}P < .01$, $^{***}P < .001$, $^{****}P < .0001$). Abbreviations: ADCD, antibody-dependent complement deposition; ADCP, antibody-dependent cellular phagocytosis; ADNP, antibody-dependent neutrophil phagocytosis; CSF, cerebrospinal fluid; HIV, human immunodeficiency virus; IFN-γ, interferon-γ; NK, natural killer; ns, not statistically significant.

functional antibody subclasses in humans [29], we hypothesized that the CSF, enriched in our study of these 2 IgG subclasses, would harbor robust antibody effector functions. However, HIV-specific antibodies in CSF exhibited little to no function compared to plasma antibodies (Figure 3A and 3B), with notably lower levels of ADCD and ADNP in CSF (Figure 3B). This reduced functionality was linked to lower binding to both activating (FcγR2A, 3A, 3B) and inhibitory (FcγR2B) FcRs, at similar levels across all HIV antigens (gp120, gp140, p24) (Figure 3C and 3D). These data point to the selective transfer of IgG1 and IgG3 antibodies with attenuated Fc-effector functions into the CNS, possibly reflecting exclusion of functional antibodies aimed at protecting the brain from potentially pathological antibodies. Along these lines, complement activation has been implicated in brain tissue damage in some acute infectious encephalitis [30–32], but is not observed in other chronic conditions [33], suggesting that ADCD-inducing antibodies may penetrate the brain only under particular conditions, and are otherwise excluded from the brain antibody arsenal during infections marked by persistent low-level viral replication, such as HIV infection of the CNS.

Defining Multivariate Compartment-Specific Antibody Profiles and Functional Coordination

To define the features that distinguished plasma- and CSF-antibodies, we next applied multivariate models (LASSO/PLSDA) to all combined HIV-specific antibody data [21]. Clear separation was observed between plasma and CSF antibody profiles (Figure 4A; model validation $P < .01$, accuracy 100%). In agreement with the univariate analysis, gp120-specific ADCP, ADCD, and FcRs binding (particularly, FcγR2B and FcRn) were enriched in plasma (Figure 4B). These data clearly demonstrate the exclusion of functional antibodies

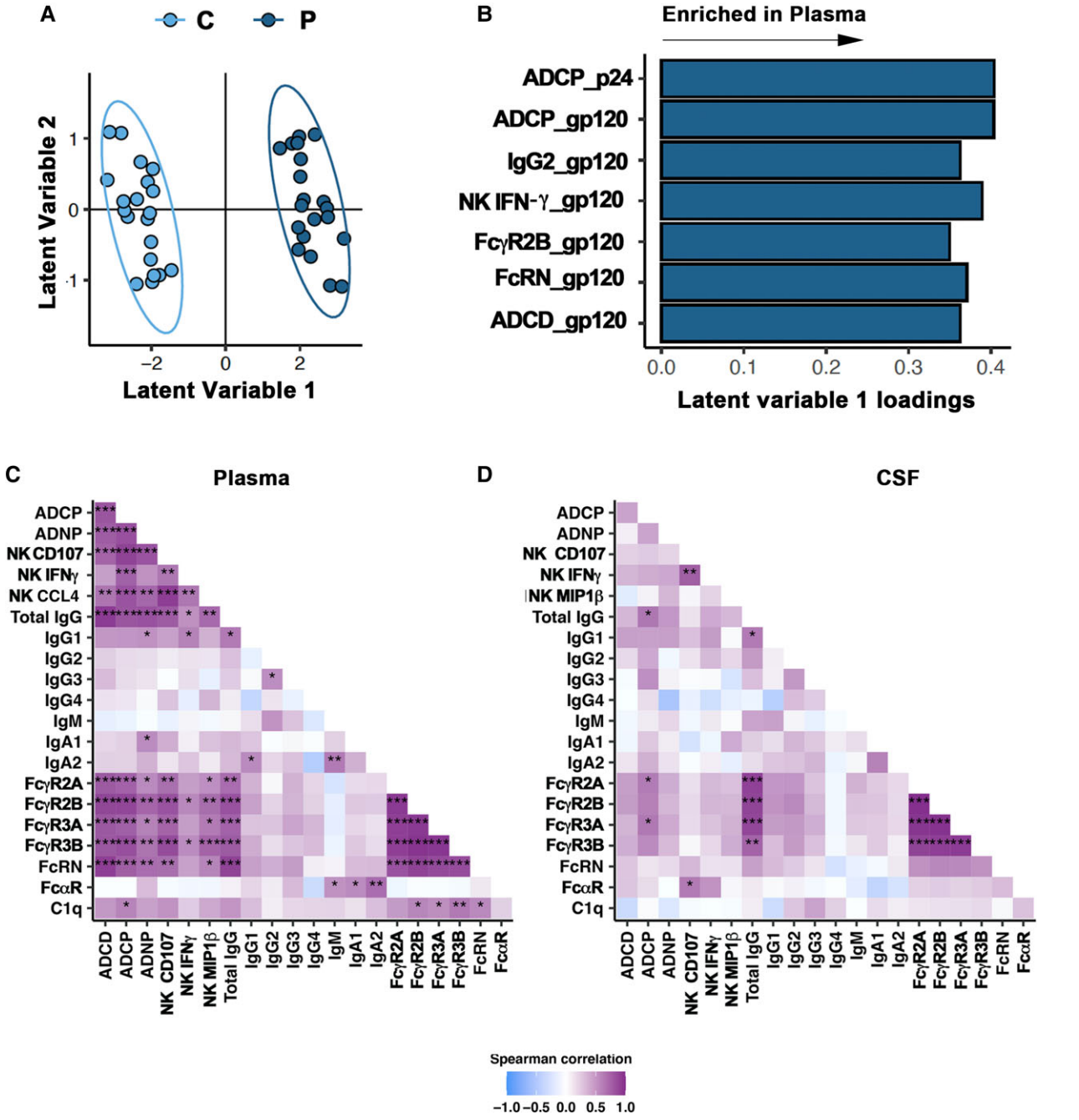

Figure 4. Multivariate antibody signatures and functional correlations across plasma and CSF. *A* and *B*, Multivariate analysis of antibody signatures in plasma and CSF. M-PLSDA on LASSO-selected features was used to resolve antibody profiles in plasma:CSF pairs. Dots represent individual samples (plasma [P] CSF [C]) across all 3 HIV antigens (gp120, gp140, p24). Five-fold cross validation was performed, resulting in 100% cross-validation accuracy. Bar graph shows LASSO-selected features across all 3 HIV antigens (gp120, gp140, p24) ranked by their variable importance in projection. All selected features are enriched in plasma. *C* and *D*, Correlation matrix across gp120-specific antibody functions (ADCD, ADCP, ADNP, NK CD107, NK IFN-γ, NK CCL4) Ig classes and subclasses (total IgG, IgG1, IgG2, IgG3, IgG4, IgM, IgA1, IgA2), and Fc receptor binding (FcγR2A, FcγR2B, FcγR3A, FcγR3B, FcRn, FcαR, C1q) in plasma and CSF where correlation strength is proportional to color intensity (*r* from −1 = negative correlation, blue to 1 = positive correlation, purple). Z-scores, Spearman *r* test, Benjamini-Hochberg correction for multiple comparisons; $^{*}P < .05$, $^{**}P < .01$, $^{***}P < .001$. Abbreviations: ADCD, antibody-dependent complement deposition; ADCP, antibody-dependent cellular phagocytosis; ADNP, antibody-dependent neutrophil phagocytosis; CSF, cerebrospinal fluid; HIV, human immunodeficiency virus; IFN-γ, interferon-γ; Ig, immunoglobulin; LASSO, least absolute shrinkage selection operator; M-PLSDA, multilevel partial least square discriminant analysis; NK, natural killer.

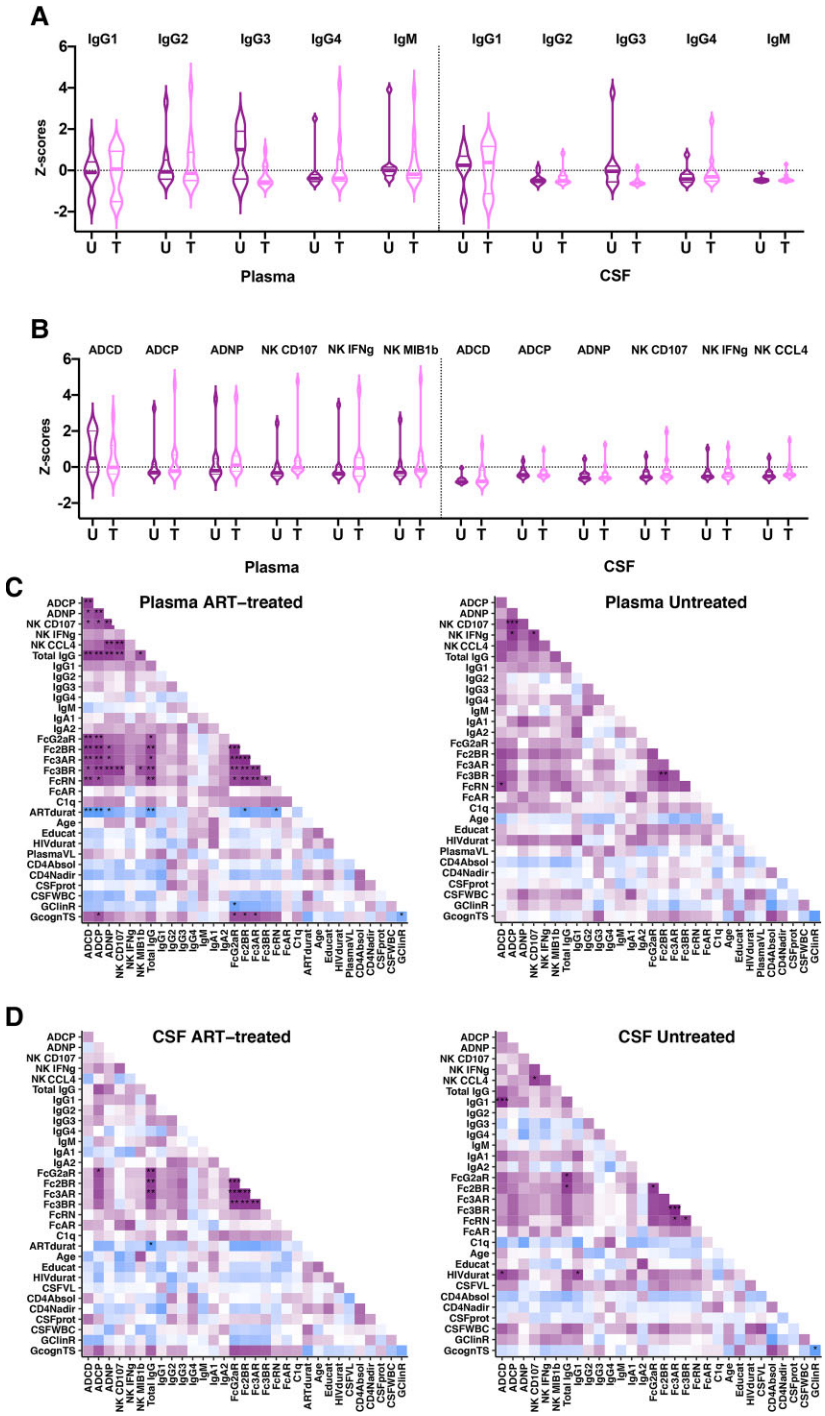

Figure 5. Effect of ART treatment on antibody profiles in plasma and CSF. *A*, Violin plots of IgG subclasses and IgM in plasma and CSF, comparing ART-treated and untreated individuals. *B*, Violin plots of antibody functions in plasma and CSF, comparing ART-treated and untreated individuals. *A* and *B*, Normalized values, Z-scores, Friedman test with Dunn correction, $P > .05$. *C* and *D*, Correlation matrix between clinical variables (age, years of education, duration of HIV infection, plasma HIV load, CSF HIV load, count of $CD4^+$ T cells/mL in blood at the time of sample, nadir of $CD4^+$ T-cell count, total protein mg/dL in CSF, white blood cells/mL in CSF, Global Clinical Rating, Global Cognitive T-scores) and gp120-specific antibody features (Ig classes [IgG, IgM, IgA], Ig subclasses [IgG1, IgG2, IgG3, IgG4, IgA1, IgA2], functions [ADCD, ADCP, ADNP, NK CD107, NK IFN-γ, NK CCL4], and Fc receptor binding [Fcγ2A, Fcγ2B, Fcγ3A, Fcγ3B, FcRn, FcαR, C1q]) in plasma and CSF of ART-treated versus untreated individuals, where correlation strength is proportional to color intensity: *r* from −1 = negative correlation, blue to 1 = positive correlation, purple. Z-scores, Spearman *r* test, Benjamini-Hochberg correction for multiple comparisons, $*P < .05$, $**P < .01$, $***P < .001$. Abbreviations: ADCD, antibody-dependent complement deposition; ADCP, antibody-dependent cellular phagocytosis; ADNP, antibody-dependent neutrophil phagocytosis; ART, antiretroviral therapy; CD4Absol, count of $CD4^+$ T cells/mL in blood at the time of sample; CD4Nadir, nadir of $CD4^+$ T cells count; CSF, cerebrospinal fluid; CSFprot, total protein mg/dL in CSF; CSFVL, CSF HIV load; CSFWBC, white blood cells/mL in CSF; Educat, years of education; GClinR, Global Clinical Rating; GcognTS, Global Cognitive T-scores; HIV, human immunodeficiency virus; HIVdurat, duration of HIV infection; IFN-γ, interferon-γ; Ig, immunoglobulin; NK, natural killer; PlasmaVL, plasma HIV load; T, ART-treated; U, untreated.

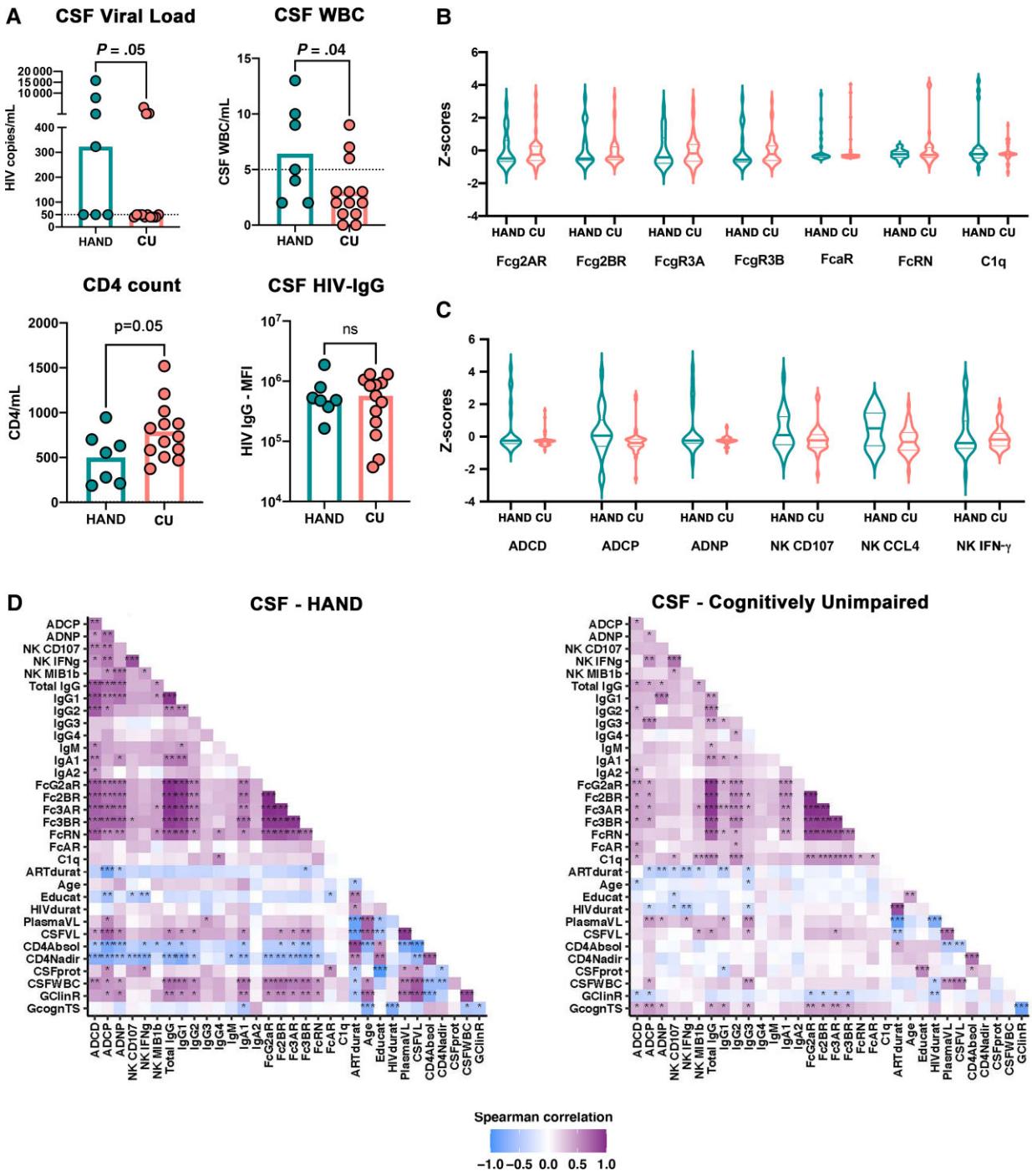

Figure 6. CSF-antibody signatures in HAND. *A*, Dot-bar plot showing CSF-HIV load (expressed as number of copies/mL), CSF leukocytes count, blood $CD4^+$ T-cell count (expressed as number of $CD4^+$ cells/mL), and CSF-HIV-specific IgG titers in HAND (green) versus cognitively unimpaired (salmon) individuals. Mann-Whitney test. *B* and *C*, Violin plots of FcR binding and functions in CSF, comparing HAND (green) and cognitively unimpaired (salmon) individuals. Z-scores, Friedman test with Dunn correction, $P > .05$. *D*, Correlation matrix of gp120-specific functions (ADCD, ADCP, ADNP, NK CD107, NK IFN-γ, NK CCL4) Ig classes and subclasses (total IgG, IgG1, IgG2, IgG3, IgG4, IgM, IgA1, IgA2), Fc receptor binding (FcγR2A, FcγR2B, FcγR3A, FcγR3B, FcRn, FcαR, C1q), and clinical variables (duration of ART treatment, age, years of education, estimated duration of HIV, plasma HIV load, CSF HIV load, $CD4^+$ T cell-count at time of sample, $CD4^+$ T-cell count at nadir, CSF total protein level, CSF white blood cell count/mL, Global Cognitive Rating [higher levels indicate higher cognitive impairment], Global Cognitive T-Scores [higher levels indicate lower cognitive impairment]) in CSF of HAND and CN individuals. Correlation strength is proportional to color intensity: *r* from −1 = negative correlation, blue to 1 = positive correlation, purple). Z-scores, Spearman *r* test, Benjamini-Hochberg correction for multiple comparisons, $*P < .05$, $**P < .01$, $***P < .001$. Abbreviations: ADCD, antibody-dependent complement deposition; ADCP, antibody-dependent cellular phagocytosis; ADNP, antibody-dependent neutrophil phagocytosis; ARTdurat, duration of ART treatment; CD4Nadir, $CD4^+$ T-cell count at nadir; CSF, cerebrospinal fluid; CSFprot, CSF total protein level; CSFVL, CSF HIV load; CSFWBC, CSF white blood cell count/mL; CU, cognitively unimpaired; educat, years of education; GClinR, Global Cognitive Rating; GCognTS, Global Cognitive T-Scores; HAND, HIV-associated neurocognitive disorder; HIV, human immunodeficiency virus; HIVdurat, estimated duration of HIV; IFN-γ, interferon-γ; Ig, immunoglobulin; MFI, median fluorescence intensity; NK, natural killer; ns, not statistically significant; PlasmaVL, plasma HIV load; WBC, white blood cell.

from the CSF, far beyond our traditional understanding of isotype/subclass sieving into this unique compartment.

Also, we explored the coordination between HIV-specific antibody functions, isotypes, subclasses, and FcR binding. While antibody responses were highly correlated in plasma, CSF antibodies exhibited lower coordination in all but FcR binding profiles (Figure 4C and 4D). These data further highlight the presence of different qualities of antibodies across compartments, and the sieving of antibodies from the periphery, rather than local production of antibodies in the CNS that would be anticipated to exhibit a broader and more coordinated functional profile.

ART Treatment Results in a More Strongly Coordinated HIV-Specific Plasma Antibody Response

Previous studies have shown that ART induces a strongly coordinated humoral immune response, potentially linked to reduced immune activation in the setting of lower viremia [34]. Whether ART also affects humoral responses in the CSF remains unclear. Here, we compared antibody profiles, viral markers, and clinical features in plasma and CSF across the 11 virally suppressed ART-treated and 9 ART-naive individuals (Table 1). As expected, untreated individuals exhibited higher viral loads in both plasma and CSF and lower $CD4^+$ counts in blood. Additionally, untreated individuals had higher leukocyte counts in the CSF, suggesting persistent neuroinflammation. Otherwise, no differences in neurocognitive scores (Table 1), Ig isotype/subclass distribution (Figure 5A), function (Figure 5B), and FcR binding (not shown) were observed between treated and untreated individuals. As previously reported [34, 35], enhanced HIV-specific antibody functional coordination in the plasma was observed in the ART-treated compared to untreated individuals (Figure 5C). In contrast, in the CSF, antibody functional coordination remained low and more variable, regardless of ART treatment (Figure 5D), suggesting functional segregation of antibody effector profiles across the compartments even in the setting of successful ART. Thus, these data suggest that ART-induced reduction in peripheral immune activation may enhance systemic humoral coordination, but may have a more limited effect on CSF antibody profiles.

HAND Is Associated With Higher Viral Burden, Neuroinflammation, and Antibody Functional Coordination

We next aimed to define the relationship between viral burden or antibody features and HAND (Supplementary Table). Individuals with HAND exhibited higher CSF HIV loads and leukocyte counts (Figure 6A), suggesting a role for CNS viral burden and neuroinflammation in the development of neurocognitive dysfunction, as supported by previous studies [11, 36, 37], even in some persons with milder forms (ANI and MND). As expected, we observed a relationship between low blood $CD4^+$ counts and presence of HAND (Figure 6A) [38, 39], likely reflecting advanced HIV disease. Additionally, a logistic regression model with HAND as the outcome and ART along with antibody features as predictors suggested ART was not a significant predictor of HAND status ($P = .99$), in accordance with univariate analysis (Supplemental Table). Interestingly, while there were no significant differences in antibody titers, FcR binding, and function between cognitively unimpaired and impaired individuals in plasma and CSF (Figure 6B and 6C, and Supplementary Figure 2), coordination of FcR binding, antibody titers, and functions were higher in the CSF of individuals with HAND compared to cognitively unimpaired individuals (Figure 6D), pointing to an inflammatory shift in antibody profiles within the brain of cognitively impaired individuals. Whether this coordination results in distinct inflammatory cascades within the CNS compartment that contributes to progressive neuroimpairment remains unclear but could provide insights into possible mechanisms to prevent or delay HAND.

DISCUSSION

There is increasing evidence that humoral responses, in particular highly functional antibodies, are important correlates of HIV viral control [16, 40]. These responses have been well-established in the peripheral blood. However, whether these antibodies can transit to the CNS or other privileged sites where the virus can escape traditional immune control remains unclear. Thus, to begin to define the nature of antibody transfer to the CNS, we deeply profiled the humoral immune response across plasma and CSF in a cohort of ART-treated and untreated persons with HIV. Striking compartmentalization was observed in antibody profiles, marked by a unique and highly selective enrichment of poorly functional IgG1 and IgG3 antibodies in the CSF. Moreover, HIV-specific antibodies were transferred at higher levels than antibodies to other pathogens. Given that FcRn is unlikely to bind and selectively transport antibodies with low Fc-effector functions, these data suggest that an alternative transfer mechanism may contribute to antibody crossing through the BBB that is augmented in the setting of HIV infection. Thus, this study provides previously unappreciated insights into antibody transfer to the brain that may support the design of future therapeutic interventions to cure HIV and other infections in the CNS.

If B cells were producing HIV-specific antibodies locally in the CNS, they would switch and produce multiple antibody isotypes or subclasses. Instead, in our study we observed a striking sieving across the BBB, marked by selection of IgG1 and IgG3 in the CSF for both HIV and non-HIV–specific antibodies. Given enhanced affinity of FcRn for IgGs, with marked transfer efficiency differences across subclasses (IgG1 > IgG3 > IgG2) [28, 29], these data are consistent with an FcRn-mediated

transfer mechanism across the BBB. However, the highly selective exclusion of FcγR-binding and functional antibodies suggests sieving mechanisms beyond FcRn. For instance, FcRn may act with other Fc-receptors at the BBB or other barriers. Along these lines, recent data showed collaboration between FcγR3a and FcRn in the placenta [19, 41], to ensure selection of optimal IgG, or to restrict passage of inflammatory antibodies that could otherwise cause localized pathology. Alternatively, selective exclusion of inflammatory IgGs from the brain may also occur via enzymatic modification of Fc-glycosylation of CSF antibodies, as documented in the liver [42]. However, whether similar mechanisms are at play in the CNS or whether a noncanonical Fc-receptor may work in concert with FcRn to selectively enrich less inflammatory antibodies in the brain is unclear.

During early infection, anti-HIV humoral responses evolve within 2–3 weeks after initial virus entry [43], with antibody levels increasing earlier in the blood than in CSF [10]. During chronic infection, ART treatment results in a significant decrease in HIV loads [44], systemic immune activation [45], and systemic antibody levels [46]. However, whether ART has similar effects in the CSF compartment remains a matter of debate. In our study, we did not observe differences in antibody titers, IgG subclasses, functions, or FcγR binding of CSF-antibodies between treated and untreated individuals. However, while coordination of antibody effector functions improved in the peripheral circulation with ART, the same improvement in antibody function was not observed in the CSF. These data highlight the persistent dysfunction in the CSF, which may relate to reduced ART activity in the CNS. These results are in line with recent observations that in chronically infected patients, ART does not significantly affect CSF antibody levels [10], and highlights that HIV-specific antibody quality may in fact reflect persistent viral load in the CNS.

HAND remains one of the main drivers of poor quality of life in people living with HIV, and its pathogenesis is multifactorial [36]. Our study supports a role of HIV infection of the CNS and neuroinflammation, even in some individuals with only mildly impaired cognition (ANI and MND), by showing a direct correlation between severity of cognitive impairment, level of HIV replication in CSF, and neuroinflammation, indicated by an increased number of infiltrating leukocytes in CSF. This is in line with other studies reporting elevated inflammatory brain metabolites [47, 48] and white matter changes in HIV-infected individuals with more severe forms of HAND [49]. However, our observation that antibody titers and Fc-effector functions did not correlate with severity of HAND suggests that antibody-mediated innate immune functions are not likely to be major contributors to HAND pathogenesis.

The current study has several limitations, including the small cross-sectional sample size, which limited statistical power to perform subgroup analyses, such as the comparison of HAND severity by ART treatment. Additionally, the study lacked information on oligoclonal bands in the CSF to support either the selective antibody-transfer across the BBB or the potential for intrathecal antibody synthesis. Also, we did not perform genetic analyses of HIV in the blood and CSF to support the role of compartmentalized immune responses in the emergence/selection of unique CNS HIV variants that might contribute to HAND pathogenesis [50]. Nevertheless, our study provides the first functional characterization of brain-specific HIV antibody signatures in the CNS, suggesting a unique compartmentalization of the anti-HIV humoral response during chronic infection. The selective sieving of antibodies with reduced functionality might help to prevent pathology within the brain, but may also allow the virus to persist unrestricted by traditional antiviral immune mechanisms. These novel observations highlight the importance of deeper longitudinal analyses of antibody trafficking to the brain in HIV and across neuroinfections and could provide critical insights for the design of next-generation therapeutics that can gain access to the brain through mechanisms that go beyond FcRn-mediated transfer to selectively target and eliminate viruses from this immune-privileged site.

Supplementary Data

Supplementary materials are available at *The Journal of Infectious Diseases* online (http://jid.oxfordjournals.org/). Supplementary materials consist of data provided by the author that are published to benefit the reader. The posted materials are not copyedited. The contents of all supplementary data are the sole responsibility of the authors. Questions or messages regarding errors should be addressed to the author.

Notes

Author contributions. M. S., D. G., and G. A. conceived and designed the experiments. M. S., S. S., and Y. D. performed the experiments. M. S., D. C., C. L., and D. A. L. analyzed the data. M. S., D. C., C. L., M. J. G., E. R., N. W., S. S. M., D. G., and G. A. contributed to interpretation of data. M. S. and G. A. wrote the paper. All authors revised the paper for intellectual content.

Financial support. This study was supported by the American Academy of Neurology (Neuroscience Research Scholarship to M. S.); the Swiss National Science Foundation (to M. S.); Nancy Zimmerman; Mark and Lisa Schwartz; an anonymous donor; Terry and Susan Ragon; the SAMANA Kay MGH Research Scholars Award; the Ragon Institute of MGH, MIT and Harvard, Massachusetts Consortium on Pathogen Readiness; National Institutes of Health (NIH; grant numbers 3R37AI080289-11S1, R01AI146785, U19AI42790-01, U19AI135995-02, 1U01CA260476-01, and CIVIC75N93019C00052); Gates Foundation Global Health Vaccine Accelerator Platform (grant numbers OPP1146996 and INV-001650); the Musk Foundation; and the Executive

Committee on Research of Massachusetts General Hospital (grant numbers 230598 to G. A.; R56 MH115853 to D. G.; and NIH K23MH115812-01 to S. M.). NNTC sites were supported by National Institute of Mental Health (NIMH) and National Institute of Neurological Disorders and Stroke (NINDS; grant numbers U24MH100931, U24MH100930, U24MH100929, U24MH100928, and U24MH100925). CHARTER sites were supported by NIMH/NINDS (grant numbers HHSN271201000036C and HHSN271201000030C). Funding to pay the Open Access publication charges for this article was provided by NIH R01AI146785.

Potential conflicts of interest. G. A. is a founder of SeromYx Systems. All other authors report no potential conflicts. All authors have submitted the ICMJE Form for Disclosure of Potential Conflicts of Interest. Conflicts that the editors consider relevant to the content of the manuscript have been disclosed.

References

1. Blankson JN, Persaud D, Siliciano R. The challenge of viral reservoirs in HIV-1 infection. Annu Rev Med **2002**; 53: 557–93.
2. Farhadian SF, Mistry H, Kirchwey T, et al. Markers of CNS injury in adults living with HIV with CSF HIV not detected vs detected <20 copies/mL. Open Forum Infect Dis **2019**; 6:ofz528.
3. Tambussi G, Gori A, Capiluppi B, et al. Neurological symptoms during primary human immunodeficiency virus (HIV) infection correlate with high levels of HIV RNA in cerebrospinal fluid. Clin Infect Dis **2000**; 30:962–5.
4. Dahl V, Peterson J, Fuchs D, Gisslen M, Palmer S, Price RW. Low levels of HIV-1 RNA detected in the cerebrospinal fluid after up to 10 years of suppressive therapy are associated with local immune activation. AIDS **2014**; 28: 2251–8.
5. Edén A, Marcotte TD, Heaton RK, et al. Increased intrathecal immune activation in virally suppressed HIV-1 infected patients with neurocognitive impairment. PLoS One **2016**; 11:e0157160.
6. Shebl FM, Yu K, Landgren O, Goedert JJ, Rabkin CS. Increased levels of circulating cytokines with HIV-related immunosuppression. AIDS Res Hum Retroviruses **2012**; 28:809–15.
7. Imami N, Antonopoulos C, Hardy GA, Gazzard B, Gotch FM. Assessment of type 1 and type 2 cytokines in HIV type 1-infected individuals: impact of highly active antiretroviral therapy. AIDS Res Hum Retroviruse **1999**; 15: 1499–508.
8. Relucio KI, Beernink HT, Chen D, Israelski DM, Kim R, Holodniy M. Proteomic analysis of serum cytokine levels in response to highly active antiretroviral therapy (HAART). J Proteome Res **2005**; 4:227–31.
9. Rahimy E, Li F-Y, Hagberg L, et al. Blood-brain barrier disruption is initiated during primary HIV infection and not rapidly altered by antiretroviral therapy. J Infect Dis **2017**; 215:1132–40.
10. Burbelo PD, Price RW, Hagberg L, et al. Anti-human immunodeficiency virus antibodies in the cerebrospinal fluid: Evidence of early treatment impact on central nervous system reservoir? J Infect Dis **2018**; 217:1024–32.
11. Heaton RK, Clifford DB, Franklin DR, et al. HIV-associated neurocognitive disorders persist in the era of potent antiretroviral therapy. CHARTER Study. Neurology **2010**; 75:2087–96.
12. Antinori A, Arendt G, Becker JT, et al. Updated research nosology for HIV-associated neurocognitive disorders. Neurology **2007**; 69:1789–99.
13. Blackstone K, Moore DJ, Franklin DR, et al. Defining neurocognitive impairment in HIV: deficit scores versus clinical ratings. Clin Neuropsychol **2012**; 26:894–908.
14. Brown EP, Licht AF, Dugast A-S, et al. High-throughput, multiplexed IgG subclassing of antigen-specific antibodies from clinical samples. J Immunol Methods **2012**; 386: 117–23.
15. McAndrew EG, Dugast A-S, Licht AF, Eusebio JR, Alter G, Ackerman ME. Determining the phagocytic activity of clinical antibody samples. J Vis Exp **2011**; 57:e3588.
16. Ackerman ME, Moldt B, Wyatt RT, et al. A robust, high-throughput assay to determine the phagocytic activity of clinical antibody samples. J Immunol Methods **2011**; 366: 8–19.
17. Barouch DH, Alter G, Broge T, et al. Protective efficacy of adenovirus/protein vaccines against SIV challenges in rhesus monkeys. Science **2015**; 349:320–4.
18. Fischinger S, Fallon JK, Michell AR, et al. A high-throughput, bead-based, antigen-specific assay to assess the ability of antibodies to induce complement activation. J Immunol Methods **2019**; 473:112630.
19. Jennewein MFM, Goldfarb I, Dolatshahi S, et al. Fc glycan-mediated regulation of placental antibody transfer. Cell **2019**; 178:202–15.e14.
20. Chung AW, Ghebremichael M, Robinson H, et al. Polyfunctional Fc-effector profiles mediated by IgG subclass selection distinguish RV144 and VAX003 vaccines. Sci Transl Med **2014**; 6:228ra38.
21. Westerhuis JA, van Velzen EJJ, Hoefsloot HCJ, Smilde AK. Multivariate paired data analysis: multilevel PLSDA versus OPLSDA. Metabolomics **2010**; 6:119–28.
22. Dickinson BL, Badizadegan K, Wu Z, et al. Bidirectional FcRn-dependent IgG transport in a polarized human intestinal epithelial cell line. J Clin Invest **1999**; 104:903–11.
23. Claypool SM, Dickinson BL, Wagner JS, et al. Bidirectional transepithelial IgG transport by a strongly polarized

basolateral membrane Fcγ-receptor. Mol Biol Cell **2004**; 15:1746–59.
24. Schlachetzki F, Zhu C, Pardridge WM. Expression of the neonatal Fc receptor (FcRn) at the blood-brain barrier. J Neurochem **2002**; 81:203–6.
25. Serafini B, Rosicarelli B, Magliozzi R, Stigliano E, Aloisi F. Detection of ectopic B-cell follicles with germinal centers in the meninges of patients with secondary progressive multiple sclerosis. Brain Pathol **2004**; 14:164–74.
26. Steere AC, Berardi VP, Weeks KE, Logigian EL, Ackermann R. Evaluation of the intrathecal antibody response to *Borrelia burgdorferi* as a diagnostic test for Lyme neuroborreliosis. J Infect Dis **1990**; 161:1203–9.
27. Weber MS, Hemmer B, Cepok S. The role of antibodies in multiple sclerosis. Biochim Biophys Acta Mol Basis Dis **2011**; 1812:239–45.
28. Piche-Nicholas NM, Avery LB, King AC, et al. Changes in complementarity-determining regions significantly alter IgG binding to the neonatal Fc receptor (FcRn) and pharmacokinetics. MAbs **2018**; 10:81–94.
29. Vidarsson G, Dekkers G, Rispens T. IgG subclasses and allotypes: from structure to effector functions. Front Immunol **2014**; 5:520.
30. Ernst JD, Hartiala KT, Goldstein IM, Sande MA. Complement (C5)-derived chemotactic activity accounts for accumulation of polymorphonuclear leukocytes in cerebrospinal fluid of rabbits with pneumococcal meningitis. Infect Immun **1984**; 46:81–6.
31. Mook-Kanamori BB, Brouwer MC, Geldhoff M, van der Ende A, van de Beek D. Cerebrospinal fluid complement activation in patients with pneumococcal and meningococcal meningitis. J Infect **2014**; 68:542–7.
32. Rupprecht TA, Angele B, Klein M, et al. Complement C1q and C3 are critical for the innate immune response to *Streptococcus pneumoniae* in the central nervous system. J Immunol **2007**; 178:1861–9.
33. Martinez-Hernandez E, Horvath J, Shiloh-Malawsky Y, Sangha N, Martinez-Lage M, Dalmau J. Analysis of complement and plasma cells in the brain of patients with anti-NMDAR encephalitis. Neurology **2011**; 77:589–93.
34. Ackerman ME, Mikhailova A, Brown EP, et al. Polyfunctional HIV-specific antibody responses are associated with spontaneous HIV control. PLoS Pathog **2016**; 12: e1005315.
35. Das J, Devadhasan A, Linde C, et al. Mining for humoral correlates of HIV control and latent reservoir size. PLOS Pathog **2020**; 16:e1008868.
36. Hong S, Banks WA. Role of the immune system in HIV-associated neuroinflammation and neurocognitive implications. Brain Behav Immun **2015**; 45:1–12.
37. McCombe JA, Vivithanaporn P, Gill MJ, Power C. Predictors of symptomatic HIV-associated neurocognitive disorders in universal health care. HIV Med **2013**; 14: 99–107.
38. Marcotte TD, Deutsch R, McCutchan JA, et al. Prediction of incident neurocognitive impairment by plasma HIV RNA and CD4 levels early after HIV seroconversion. Arch Neurol **2003**; 60:1406–12.
39. Ellis RJ, Badiee J, Vaida F, et al. CD4 nadir is a predictor of HIV neurocognitive impairment in the era of combination antiretroviral therapy. AIDS **2011**; 25:1747–51.
40. Chung AW, Mabuka JM, Ndlovu B, et al. Viral control in chronic HIV-1 subtype C infection is associated with enrichment of p24 IgG1 with Fc effector activity. AIDS **2018**; 32:1207–17.
41. Atyeo C, Pullen KM, Bordt EA, et al. Compromised SARS-CoV-2-specific placental antibody transfer. Cell **2021**; 184:628–42.e10.
42. Jones MB, Oswald DM, Joshi S, Whiteheart SW, Orlando R, Cobb BA. B-cell-independent sialylation of IgG. Proc Natl Acad Sci USA **2016**; 113:7207–12.
43. Cohen MS, Gay CL, Busch MP, Hecht FM. The detection of acute HIV infection. J Infect Dis **2010**; 202:S270–7.
44. Phillips AN, Staszewski S, Weber R, et al. HIV viral load response to antiretroviral therapy according to the baseline CD4 cell count and viral load. JAMA **2001**; 286:2560.
45. Hileman CO, Funderburg NT. Inflammation, immune activation, and antiretroviral therapy in HIV. Curr HIV/AIDS Rep **2017**; 14:93–100.
46. Eshleman SH, Laeyendecker O, Kammers K, et al. Comprehensive profiling of HIV antibody evolution. Cell Rep **2019**; 27:1422–33.e4.
47. Sailasuta N, Ross W, Ananworanich J, et al. Change in brain magnetic resonance spectroscopy after treatment during acute HIV infection. PLoS One **2012**; 7:e49272.
48. Valcour V, Chalermchai T, Sailasuta N, et al. Central nervous system viral invasion and inflammation during acute HIV infection. J Infect Dis **2012**; 206:275–82.
49. Wright PW, Vaida FF, Fernández RJ, et al. Cerebral white matter integrity during primary HIV infection. AIDS **2015**; 29:433–42.
50. Schnell G, Price RW, Swanstrom R, Spudich S. Compartmentalization and clonal amplification of HIV-1 variants in the cerebrospinal fluid during primary infection. J Virol **2010**; 84:2395–407.